Published by Institute of Physics Publishing for SISSA

Received: *November 11, 2005*
Revised: *February 10, 2006*
Accepted: *February 18, 2006*
Published: *March 2, 2006*

Exploring topology conserving gauge actions for lattice QCD

Wolfgang Bietenholz,[a] **Karl Jansen,**[b] **Kei-Ichi Nagai,**[bc] **Silvia Necco,**[de] **Luigi Scorzato**[a] **and Stanislav Shcheredin**[f]

[a] *Institut für Physik, Humboldt Universität zu Berlin*
Newtonstr. 15, D-12489 Berlin, Germany
[b] *NIC, DESY*
Platanenallee 6 D-15738 Zeuthen, Germany
[c] *Fachbereich Physik, Universität Wuppertal*
Gauss-Str. 20, D-42119 Wuppertal, Germany
[d] *Centre de Physique Théorique*
Luminy, Case 907, F-13288, Marseille Cedex 9, France
[e] *IFIC - Instituto de Fisica Corpuscular Edificio Institutos de Investigacion*
Apartado de Correos 22085 E-46071 Valencia, Spain
[f] *Fakultät für Physik, Universität Bielefeld*
D-33615 Bielefeld, Germany
E-mail: bietenho@physik.hu-berlin.de, karl.jansen@desy.de, keiichi.nagai@desy.de, necco@cpt.univ-mrs.fr, luigi.scorzato@physik.hu-berlin.de, shchered@physik.hu-berlin.de

Abstract: We explore gauge actions for lattice QCD, which are constructed such that the occurrence of small plaquette values is strongly suppressed. By choosing strong bare gauge couplings we arrive at values for the physical lattice spacings of $\mathcal{O}(0.1$ fm). Such gauge actions effectively tend to confine the Monte Carlo history to a single topological sector. This topological stability facilitates the collection of a large set of configurations in a specific sector, which is profitable for numerical studies in the ϵ-regime. The suppression of small plaquette values is also expected to be favourable for simulations with dynamical quarks. We use a local Hybrid Monte Carlo algorithm to simulate such actions, and we present numerical results for the static potential, the physical scale, the topological stability and the condition number of the kernel of the overlap Dirac operator. In addition we discuss the question of reflection positivity for a class of such gauge actions.

Keywords: Lattice Gauge Field Theories.

JHEP03(2006)017

Contents

1. Introduction

The standard way to formulate the QCD gauge action on a lattice is given by the *Wilson gauge action*[1][1]

$$S_{\mathrm{W}}[U] = \beta \sum_P S_P(U_P)\,, \quad S_P(U_P) = 1 - \frac{1}{3}\mathrm{Re\ Tr} U_P\ . \tag{1.1}$$

This choice is less problematic than the formulation of the fermionic part, since lattice artifacts already scale with $\mathcal{O}(a^2)$ (a is the lattice spacing), and there is no additive renormalization.

Nevertheless there are a number of suggestions for improved lattice gauge actions (for instance the tree level improved Symanzik gauge action [3], the on-shell improved Lüscher-Weisz action [4], and renormalisation group improved actions [5 – 7]). In general the goal is to further suppress the scaling artifacts by including more extended closed loops in the discrete formulation of the field strength tensor.

In the current work, instead, we look for gauge actions which suppress as far as possible the occurrence of small plaquette values. Of course, this suppression prevents the gauge field from fluctuating as it would for the Wilson gauge action, hence we have to use much stronger bare gauge couplings g_0 to arrive at a comparable lattice spacing. For practical simulations a lattice spacing of $\mathcal{O}(0.1\ \mathrm{fm})$ is required. For quenched simulations with the Wilson gauge action such a lattice spacing is obtained for $\beta = 6/g_0^2 \approx 6$. We will see that a lattice spacing of the same magnitude can still be obtained for the actions that drastically suppress small plaquette values, if we drive β down to values around and even below 1.

[1] U_P denotes the plaquette variables in a lattice gauge configurations given by the link variables $U_{x,\mu} \in \mathrm{SU}(3)$. The sum in eq. (1.1) runs over all plaquettes, see e.g. ref. [2].

JHEP03(2006)017

2. Motivations for the suppression of small plaquette values

Small plaquette values $S_P(U_P)$ are expected to be linked to small eigenvalues of the Dirac operator. Therefore, their suppression should speed up the simulation of *dynamical fermions*, and bring further improvement, in addition to recent algorithmic developments [8]. However, these properties are not tested in this work; we leave them for further investigations.

The suppression of small plaquette values should also help the computation of the overlap operator [9] – which is a solution of the Ginsparg-Wilson relation [10 – 12], $\{D, \gamma_5\} = \frac{1}{\mu} D\gamma_5 D$ (for $\mu \gtrsim 1$). The corresponding overlap operator reads

$$D_{\rm ov}(m_q) = \mu\Big(1 - \frac{m_q}{2\mu}\Big)\Big[1 + \gamma_5 Q/\sqrt{Q^2}\Big] + m_q\,, \quad Q = \gamma_5(D_{\rm W} - \mu)\,, \tag{2.1}$$

where we use lattice units ($a = 1$), $D_{\rm W}$ is the Wilson operator and m_q the quark mass. The cost of the application of $D_{\rm ov}$ essentially depends on the condition number of Q^2. This will be studied in section 4.4.

The overlap operator allows for a neat definition of the topological charge [11], through the Atiyah-Singer index: $\nu = n_+ - n_-$, where $n_\pm$ is the number of zero modes with positive/negative chirality. For independent configurations the distribution of ν is Gaussian, and its width determines the topological susceptibility.

Small plaquette values are related to the possibility of changing the topological sector. This connection was made rigorous first in ref. [13] for the overlap operator (2.1). If all the plaquette variables U_P in the configurations involved obey the inequality (at $\mu = 1$) [13, 14]

$$S_P(U_P) < \varepsilon = \frac{1}{(1 + 1/\sqrt{2})d(d-1)} \simeq \frac{1}{20.5}\,, \tag{2.2}$$

(where S_P keeps the meaning of the standard gauge action of one plaquette, as in eq. (1.1)), then the square root cannot vanish, topological transitions are excluded under continuous deformations and the topological structure is continuum-like. This constraint ensures that the spectrum of Q^2 (the argument of the square root in the overlap formula (2.1)) is strictly positive.[2] In absence of zero modes this condition also guarantees the locality of the overlap operator (in the sense of an exponential decay) [13].

A fixed topological sector in a Monte Carlo history is usually a problem. However, it can become an advantage if we want to compare lattice computation to chiral perturbation theory (χPT) in the *ϵ-regime* [16]. As opposed to the (more common) *p-regime* [17], the ϵ-regime is characterized by a correlation length $\xi = 1/m_\pi$ that exceeds the lattice size L ($\xi > L$). In this unphysical situation finite size effects are very important, but they can be related to χPT formulae. The interesting point is that these formulae involve the Low Energy Constants as they appear in infinite volume. Therefore we can extract physically relevant information even from the unphysical ϵ-regime.

What is crucial for us is that, in the ϵ-regime, observables tend to depend significantly on the topological sector, and predictions exist for expectation values in specific sectors [18].

[2] The corresponding admissibility condition has also been studied on a non-commutative torus in ref. [15].

JHEP03(2006)017

Therefore, for numerical measurements it can be advantageous, if not necessary, to disentangle the topologies, in order to extract maximal information. In this regime one would often like to collect statistics at one specific value of $|\nu|$ to measure an expectation value in this sector. For the parameters that have been used in the ϵ-regime simulations [19 – 27], it would be of particular interest to collect large sets of configurations with $|\nu| = 1$ and 2. A box with $V \approx 10$ fm^4 is suitable, but the width of the Gaussian charge distribution is then around $\langle \nu^2 \rangle \approx 10$ [21, 25]. The index measurement by itself is computationally expensive, hence identifying a set of, say, $\mathcal{O}(1000)$ configurations in one sector is a tedious task — if one uses the standard Wilson gauge action.

Therefore, it is motivated to modify the lattice gauge action such that topological transitions are suppressed. On the other hand, imposing the restrictive constraint (2.2) could cause severe practical problems. The fluctuations of the gauge field would be limited so much that one could only obtain a tiny physical lattice spacing and volume. However, even for simulations in the ϵ-regime we have to require that the spatial box length L exceeds some lower limit in the range of $L \gtrsim 1.1$ fm $\ldots$ 1.5 fm (depending on the exact criterion) [20 – 26].

Here we present numerical experiments with gauge actions which do suppress small plaquette values, but only to the extent that still allows for a reasonable physical lattice spacing to be obtained. Then there is no rigorous guarantee for topology conservation in the Monte Carlo history.[3] The hope is that the transitions are still strongly suppressed, so that the history has periods of constant charge, which are sufficiently long to allow us to collect many configurations in a specific sector. Moreover, if we can be confident that topological transitions rarely happen, most of the index computation can be omitted; one would just check after a number of configurations if the index has not changed.

These configurations should sample independently the observables to be measured in a fixed topology. Since we aim at long sequences of fixed topological charge, this can also be interpreted as a long topological autocorrelation time. Of course, at the same time, we aim at a much shorter autocorrelation time for other observables.

3. The gauge actions

We now describe a number of non-standard lattice gauge actions, which suppress the undesired small plaquette values. As long as the action for very smooth configurations — with $S_P \gtrsim 0$ for all plaquettes — is not altered, the naive continuum limit coincides with the one of the Wilson action (1.1), and with continuum QCD. The suppression becomes strong when S_P reaches the value of some parameter ε, which one would theoretically choose according to eq. (2.2). For practical purposes we will have to relax ε to larger values. A simple cutoff for S_P at this value would be conceivable, but such a discontinuity in the ac-

[3] With respect to the topological charge one could object that a Monte Carlo history proceeds in discrete jumps, so even with this constraint the charge conservation is not absolutely safe. However, this seems like a minor problem, since the charge would still be conserved over very long periods in the history, and in simulations of the HMC type the few remaining changes could be further suppressed by reducing the step size $d\tau$ (at higher cost).

JHEP03(2006)017

tion (which would then suddenly jump to infinity) does not appear promising. We can still impose a cutoff but let the plaquette action diverge continuously as S_P increases towards ε, if we modify S_P of eq. (1.1) to the hyperbolic form

$$S^{\rm hyp}_{\varepsilon,n}(U_P) = \begin{cases} \frac{S_P(U_P)}{[1-S_P(U_P)/\varepsilon]^n} & \text{for } \; S_P(U_P) < \varepsilon \\ +\infty & \text{otherwise} \end{cases} \tag{3.1}$$

for $n > 0$. This formulation, with $n = 1$, was introduced by M. Lüscher and used for conceptual studies of chiral gauge theories on the lattice [28]. In that case, ε was of course set to a theoretically stringent value.

In simulations, this action was first used in the Schwinger model by H. Fukaya and T. Onogi [29]. They set $\varepsilon = 1$, i.e. far above the theoretical value of about 0.29, but they still observed topological stability over hundreds of trajectories.[4]

The infinite part in action (3.1) means that certain steps that the HMC algorithm suggests have to be rejected for sure. Therefore we also have to verify with special care that the acceptance rate is sufficiently high. This motivated us to consider further variants of gauge actions, which also suppress the probability of plaquette actions $S_P > \varepsilon$, but which do not render a violation of this constraint completely impossible. Examples for such actions are the "power actions"and the "exponential actions",

$$S^{\rm pow}_{\varepsilon,n}(U_P) \,=\, S_P(U_P) + \frac{1}{\varepsilon} S_P(U_P)^n \,, \tag{3.2}$$

$$S^{\rm exp}_{\varepsilon,n}(U_P) \,=\, S_P(U_P) \cdot \exp\{S_P(U_P)^n/\varepsilon\} \qquad (n > 0) \;. \tag{3.3}$$

In our numerical studies we included the actions $S^{\rm hyp}_{\varepsilon,1}$ and $S^{\rm exp}_{\varepsilon,8}$. Our preliminary results were reported in refs. [30] and a comprehensive presentation will be given in the next section. Further results along these lines for quenched QCD can be found in refs. [31, 32].

A theoretical objection against the lattice action (3.1) was raised by M. Creutz [33], who observed that it does not provide a positive definite transfer matrix. By universality, we expect positivity to be restored in the continuum limit. Still, only what can be proved to hold at finite lattice spacing will certainly hold in the continuum limit. To this end we should remark that our actions at least define a positive *squared* transfer matrix. In fact for the gauge actions involved in our study "site reflection" positivity holds, since the argument given in ref. [2] (section 3.2.8) applies unchanged. From the practical point of view, the lack of positivity can be reflected in an irregular behaviour of the effective potential $V(r,t)$ at short time separation, as observed in ref. [34] for actions involving rectangular loops (like those suggested in refs. [4–6]). This is a lattice artifact which does, in principle, not constitute a problem, as long as one keeps far enough from the cutoff.[5] In the case of the actions considered in this work and with our statistical precision, such an irregular behaviour could not been observed (see subsection 4.2).

[4]Note that the factor 1/3 in the term for S_P of eq. (1.1) is actually $1/N_c$ for general SU(N_c) or U(N_c) gauge groups. Moreover, the theoretical bound for ε in $d = 2$ is a factor 6 larger than in $d = 4$, as eqs. (2.2) show (this factor is due to a summation $\sum_{\mu>\nu}$ in the term for $1/\varepsilon$).

[5]Problems can arise in the application of the variational method, where one has to choose a small reference time.

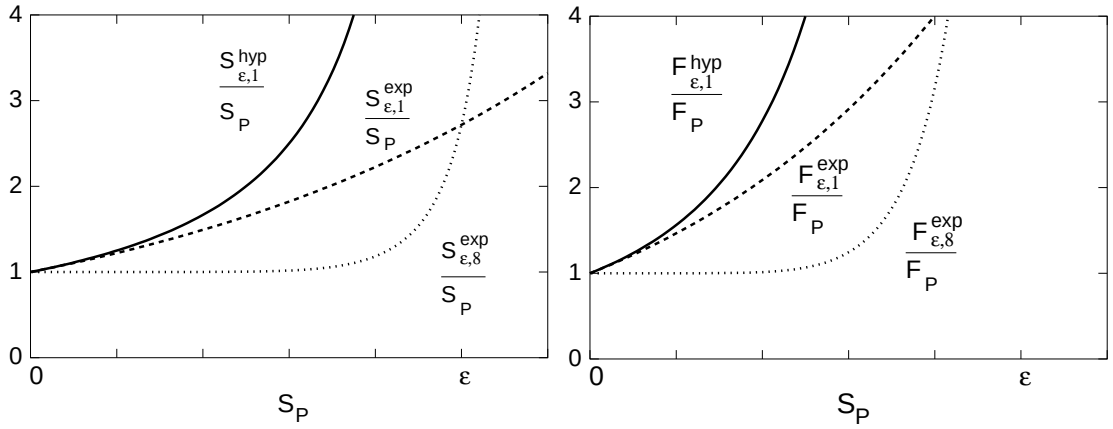

Figure 1: On the left: The ratio between the hyperbolic plaquette action (for $n = 1$) and standard plaquette action, and the corresponding ratio for the exponential actions with $n = 1$ and $n = 8$ (the latter is the case we studied). On the right: the same ratios for the HMC forces, again as a function of S_P.

4. Numerical results

Actions of the types (3.1), (3.2) and (3.3) depend non-linearly on the link variables $U_{x,\mu}$. As a consequence, the heat-bath algorithm and over-relaxation cannot be applied straightforwardly. Therefore we use the *local HMC algorithm*, which was introduced in ref. [35]. Since these actions are still composed of separate contributions by the single plaquettes, the force in the local HMC algorithm is a simple modification of the corresponding force for the Wilson action,

$$F^{\rm hyp}_{\varepsilon,n} = \frac{\delta S^{\rm hyp}_{\varepsilon,n}(U_P)}{\delta U_{x,\mu}} = F^{\rm W}(U_P) \cdot \frac{1 + \frac{n-1}{\varepsilon} S_P(U_P)}{[1 - \frac{1}{\varepsilon} S_P(U_P)]^{n+1}} \tag{4.1}$$

$$F^{\rm exp}_{\varepsilon,n} = \frac{\delta S^{\rm exp}_{\varepsilon,n}(U_P)}{\delta U_{x,\mu}} = F^{\rm W}(U_P) \cdot \left(1 + \frac{n}{\varepsilon} S_P(U_P)^{n-1}\right) \exp\left\{\frac{1}{\varepsilon} S_P(U_P)^n\right\}, \tag{4.2}$$

$$\text{where} \qquad F^{\rm W}(U_P) = \frac{\delta S_P(U_P)}{\delta U_{x,\mu}}$$

is the force of the Wilson action, and its modification by the second factor is of order $\mathcal{O}(S_P/\varepsilon)$ in both cases. This is illustrated in figure 1.

In such simulations, it is also of special importance to check that the results do not depend on the starting configuration (once we start in the desired topological sector). It would be conceivable that the constraint on the plaquette values causes also unwanted obstructions. For all the quantities to be considered below, it turned out that this was not the case; an example is discussed in subsection 4.5.

4.1 Plaquette values

As a first experiment we considered action (3.1) and searched for the lines of a constant mean plaquette action $\langle S_P \rangle$ on a 4^4 lattice, as β and the action parameter ε are varied.

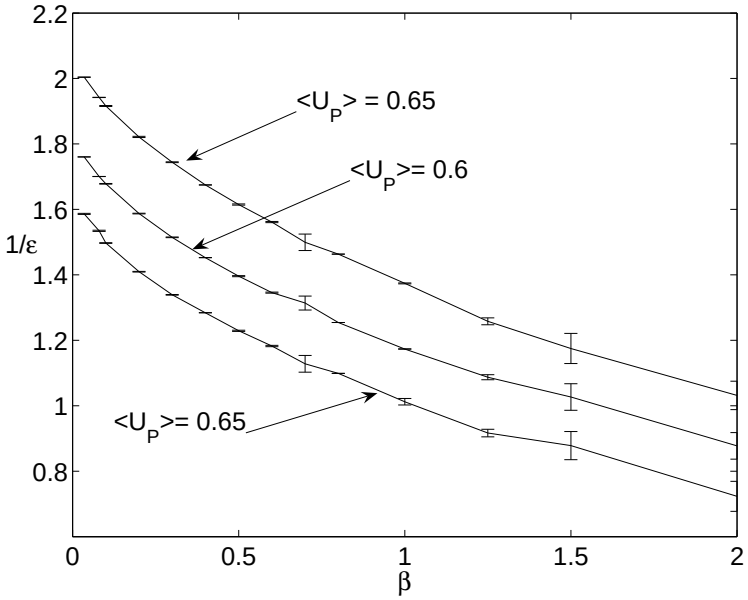

Figure 2: The lines of constant plaquette values in the plane spanned by $1/\varepsilon$ and β, on a 4^4 lattice.

The result is shown in figure 2. As we decrease ε, very small values of β, i.e. strong bare gauge couplings are needed to keep $\langle S_P \rangle$ constant. By decreasing the values of ε and β we can in fact keep $\langle S_P \rangle$ approximately constant, while drastically suppressing the occurrence of very small plaquette actions. To identify a line of a constant physics, we proceed in the next subsection to larger lattices and we consider the static potential (since the plaquette value cannot be used for this purpose).

4.2 The static potential and the physical scale

A very well established method for setting a scale in pure gauge theory is based on the measurement of the static potential at intermediate distances. This potential, and the resulting force, are extracted from the Wilson loop correlations at sufficiently large time separations, such that excited states can be neglected.

The aim is to fix the quantity $r_0 = 0.5$ fm [34] by tuning the dimensionless term

$$r^2 F(r)|_{r=r(c)} = c\,, \quad r_0 = r(1.65)\ . \tag{4.3}$$

To this end, we followed the procedure applied in refs. [36, 37], to which the reader can refer for the details of the computation.[6] The results for the action $S^{\rm hyp}_{\varepsilon,1}$ at different values of ε and β are shown in table 1. From the scale r_0/a we can identify an "equivalent" β-value for the Wilson gauge action, which we denote by $\beta_{\rm W}$. It corresponds to the same lattice spacing for the plaquette action (1.1), where we adopted the parametrisation formula in ref. [36].

[6]Note that in the present computation we did not apply the multihit procedure.

$1/\varepsilon$	β	r_0/a	β_W	$d\tau$	$\tau^{\rm plaq}$	$f_{\rm top}$	$\tau^{\rm plaq} \cdot f_{\rm top}$	acc. rate
0.	6.18	7.14(3)	6.18	0.1	7(1)	2.2(13) e-2	$\approx$ 1.5 e-1	> 99 %
1.	1.5	6.6(2)	6.13(2)	0.1	2.2(1)	3.0(23) e-3	$\approx$ 6.6 e-3	> 99 %
1.	1.5	6.6(2)	6.13(2)	0.05	2.0(1)	2.9(11) e-3	$\approx$ 5.8 e-3	> 99 %
1.	1.5	6.6(2)	6.13(2)	0.01	2.2(1)	3.5(8) e-3	$\approx$ 7.7 e-3	> 99 %
1.	1.5	6.6(2)	6.13(2)	0.005	2.3(2)	2.8(15) e-3	$\approx$ 6.4 e-3	> 99 %
1.18	1.	7.2(2)	6.18(2)	0.1	1.2(1)	2.0(12) e-3	$\approx$ 2.4 e-3	> 99 %
1.18	1.	7.2(2)	6.18(2)	0.02/0.01	1.3(1)	1.6(7) e-3	$\approx$ 2.1 e-3	> 99 %
1.25	0.8	7.0(1)	6.17(1)	0.1	1.1(1)	2.3(13) e-3	$\approx$ 2.5 e-3	> 99 %
1.52	0.3	7.3(4)	6.19(4)	0.1	0.8(1)	9.0(28) e-4	$\approx$ 7.2 e-4	≈ 95 %
1.64	0.1	6.8(3)	6.15(3)	0.1	1.0(1)	1.3(7) e-3	$\approx$ 1.3 e-3	≈ 65 %
1.64	0.1			0.05	0.7(1)	2.3(13) e-3	$\approx$ 1.6 e-3	≈ 78 %
1.64	0.1			0.025	0.6(1)	3.5(20) e-3	$\approx$ 2.1 e-3	≈ 93 %
1.64	0.1			0.001	0.5(1)	3.7(23) e-3	$\approx$ 1.9 e-3	≈ 99 %

Table 1: Results for the hyperbolic actions $S^{\rm hyp}_{\varepsilon,1}$, defined in eq. (3.1), for different values of ε and β, on a 16^4 lattice. We first show the ratio r_0/a, which fixes the physical scale. For comparison we also display the β-values $\beta_{\rm W}$, which leads to the same physical scale for the Wilson action (1.1) [36]. The trajectories were all of length 1 and divided into HMC steps of length $d\tau$. For the plaquette values this leads to a mean autocorrelation time $\tau^{\rm plaq}$, which we show as an example for the autocorrelation of a non-topological quantity. The topological stability, on the other hand, is measured by the frequency of topological transitions. More precisely, $f_{\rm top}$ is the number of topological jumps (determined from cooling), normalised by the number of trajectories. Its product with $\tau^{\rm plaq}$ characterises the dominance of the topological autocorrelation. Finally we give the acceptance rate of the local HMC algorithm. For each set of parameters in this table we collected at least 200 thermalised configurations spaced by 50 trajectories each. A detailed discussion is given in the following subsections.

$1/\varepsilon$	β	r_0/a	β_W	$d\tau$	$\tau^{\rm plaq}$	$f_{\rm top}$	$\tau^{\rm plaq} \cdot f_{\rm top}$	acc. rate
500	0.044	> 8.5	> 6.30	0.015	0.6(1)	2.5(36) e-4	$\approx$ 1.5 e-4	$\approx 99\%$
600	0.0134	8.0(2)	6.26(1)	0.015	0.6(1)	2.5(23) e-4	$\approx$ 1.5 e-4	$\approx 99\%$
1000	0.004	> 9	> 6.34	0.03	0.6(1)	0(0)		$\approx 25\%$
1000	0.00113	7.9(1)	6.25(1)	0.015	0.6(1)	1.7(23) e-4	$\approx$ 1.0 e-4	$\approx 99\%$

Table 2: Results for the exponential actions $S^{\rm exp}_{\varepsilon,8}$, defined in eq. (3.3), for different values of ε and β, on a 16^4 lattice. As in table 1 we first show the ratio r_0/a and the Wilson β-value $\beta_{\rm W}$, which leads to the same physical scale for the Wilson action (1.1) (here the finite size effects in the evaluation of r_0/a may be sizable). For different HMC steps $d\tau$ we then give the mean plaquette autocorrelation time $\tau^{\rm plaq}$, the frequency of topological transitions, $f_{\rm top}$, its product with $\tau^{\rm plaq}$ and the acceptance rate. The number of measurements for r_0/a was at least 200 in each case. Further comments are added in subsections 4.3 and 4.5.

Let us comment now on the possible errors in this evaluation:

- Previous computations [36] revealed that for a box size $L \gtrsim 3.3\ r_0$ the *finite size effects* for the computation of r_0 can be safely neglected. The same work observed

that for the Wilson action at $\beta = 5.95$ and $L \simeq 2.4\, r_0$ the finite size artifacts of the force amount to $\approx$ 3%. In our study we deal with $L = 16 \simeq (2.2 \ldots 2.4)\ r_0/a$. Hence we assume finite size effects for r_0 to be of this order as well.

- The errors quoted on r_0/a in table 1 and 2 are purely *statistical* (they were computed by the jackknife method). The same errors are shown in figure 3, which we comment on below. The extent of these errors is acceptable in this context, since a precise determination of r_0 was not the purpose of this work, so we did not aim at high statistics.

- A way to check the *lattice artifacts* is to compare the short distance force at finite lattice spacing with the one extrapolated to the continuum limit in ref. [37]. In particular we measured the ratio

$$\Delta(r/r_0) = \frac{r^2 F(r/r_0) - r^2 F(r/r_0)|_c}{r^2 F(r/r_0)|_c}\,, \tag{4.4}$$

  where $r^2 F(r/r_0)|_c$ denotes the continuum limit. The results for the action $S^{\rm hyp}_{\varepsilon,1}$ are shown in figure 3 (top). At short distances, lattice artifacts are below 15% for all the different values of $1/\varepsilon$ and β that we included. Moreover, one observes that discretisation errors grow substantially for increasing values of $1/\varepsilon$, as expected. This indicates that choosing even larger values of $1/\varepsilon$ — while keeping the physical lattice spacing fixed — could introduce sizeable cutoff effects.

- For the Wilson action it turned out that the lattice artifacts can be reduced considerably by using a so-called *"tree level improved"* definition of the force [36]. For this purpose, one defines an improved distance r_I such that the force does not contain lattice artifacts at tree level,

$$F(r_I) = \frac{4}{3}\frac{g_0^2}{4\pi r_I^2} + \mathcal{O}(g_0^4)\ . \tag{4.5}$$

  If we adapt this method, the procedure described before leads to the results shown in figure 3 (bottom). For the largest values of $1/\varepsilon$ one observes some reduction of the lattice artifacts, whereas they seem to increase for the smallest $1/\varepsilon$. This behaviour is not totally surprising, since it has been observed in other cases that this improvement is not always guaranteed [38].

  We also observe that the use of tree-level improved observables does not change the results for r_0/a itself (within the statistical errors).

- For a comparison of the scaling quality one may, for instance, refer to the Iwasaki action [5] (at $r_0/a \simeq 6.0$) and the DBW2 action [6] (at $r_0/a \simeq 5.5$) at a distance $r/r_0 \approx 0.3$: in these cases the lattice artifacts were found to be of order $\sim 10\%$ [38]. Those discretisation errors are therefore comparable to our results for the actions $S^{\rm hyp}_{\varepsilon,1}$.

JHEP03(2006)017

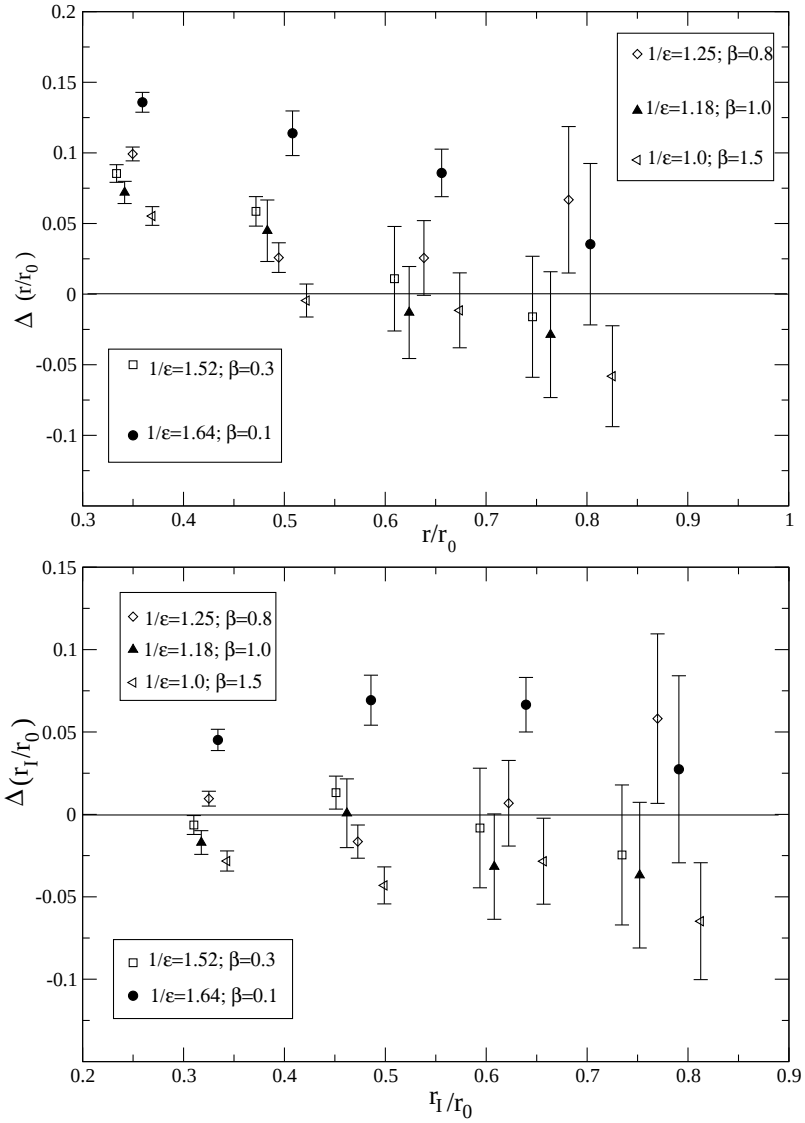

Figure 3: Lattice artifacts for the action $S^{\rm hyp}_{\varepsilon,1}$. The plots show the relative deviation of the force $r^2F(r)$ from the continuum results, given in eq. (4.4). The bottom plot uses a tree level improved definition of the force (4.5).

We repeat that our statistics is modest, and our intention in this analysis was only to check whether the errors and lattice artifacts are reasonably under control. This can be confirmed from the results shown in figure 3, and the accuracy is fully sufficient for our purposes.

4.3 Acceptance rate

Also the problem related to the acceptance rate has been mentioned in section 3. This point motivated us to consider also a set of exponential actions of the type (3.3), in addition to the hyperbolic actions, and the corresponding results are given in table 2. In both cases, the acceptance rate is very high for most of the actions we studied. It drops, however, if one pushes for very low values of ε (along with an extremely small β). As the last lines

JHEP03(2006)017

β	$1/\varepsilon$	c_2	c_6	c_{11}	c_{21}
6.17	0	1051(369)	575(110)	461(46)	390(30)
6.18	0	723(294)	501(43)	424(27)	371(16)
6.19	0	872(499)	506(57)	437(25)	374(16)
1.5	1	453(101)	360(30)	325(11)	294(7)
1	1.18	390(34)	328(18)	302(10)	281(9)
0.8	1.25	439(89)	341(23)	311(15)	285(9)
0.3	1.52	369(41)	301(13)	280(7)	263(5)
0.1	1.64	433(82)	342(18)	315(14)	293(8)

Table 3: Condition numbers c_n of the operator Q^2 in the square root of the Neuberger overlap operator at $\mu = 1.6$, after projecting out the leading $n-1$ modes of Q^2. In this comparison we always considered configurations generated by the local HMC algorithm with $d\tau = 0.1$.

in table 1 show, the acceptance rate can actually be driven up again even at $1/\varepsilon = 1.64$ by using very short HMC steps. However, this cannot be considered a solution, because it increases the costs (especially in the dynamical case), and also the frequency of topological transitions rises again (c.f. subsection 4.5). Therefore, this property sets another limit on the suppression of the small plaquette values, in addition to the scaling of the static potential at short distances.

4.4 The condition number of the kernel of the overlap operator

This subsection discusses the condition number of the operator Q^2, which is crucial for the computational effort required to deal with the overlap operator in eq. (2.1). Table 3 collects our results for the action $S^{\rm hyp}_{1,\varepsilon}$ compared to $S_{\rm W}$, at the values of ε and β corresponding to approximately constant physics according to table 1. Similar results were presented in refs. [32], which also include first tests with dynamical overlap fermions.

In our study we varied the parameter μ by units of 0.1 and found the optimal condition numbers for all gauge actions involved at $\mu = 1.6$. For the case of 10 eigenmodes of Q^2 projected out, this property can be seen in the upper plot of figure 4. Hence we compare the condition numbers at $\mu = 1.6$ for different gauge actions in table 3 and in the lower plot of figure 4. These results are based on 30 configurations in each case.

We show the condition numbers

$$c_n := \lambda_{\rm max}/\lambda_n\,, \quad (\lambda_{\rm max},\ \lambda_n\ :\ \text{largest resp. n}^{\rm th}\ \text{eigenvalue of}\ Q^2) \tag{4.6}$$

which are relevant after projecting out the leading $n-1$ modes of Q^2.[7] We see that the c_n are indeed lowered as $1/\varepsilon$ increases, which reduces the effort for overlap fermion simulations.[8]

[7] We have checked that the polynomial degree for a fixed precision of the overlap operator is $\propto \sqrt{c_n}$ (to a high precision). At the side-line, we also observed that there does not seem to be to any dependence of the condition numbers c_n on the topological sector.

[8] Alternatively, lower condition numbers c_n can also be achieved by inserting an improved kernel Q into the overlap formula, see for instance refs. [39, 25].

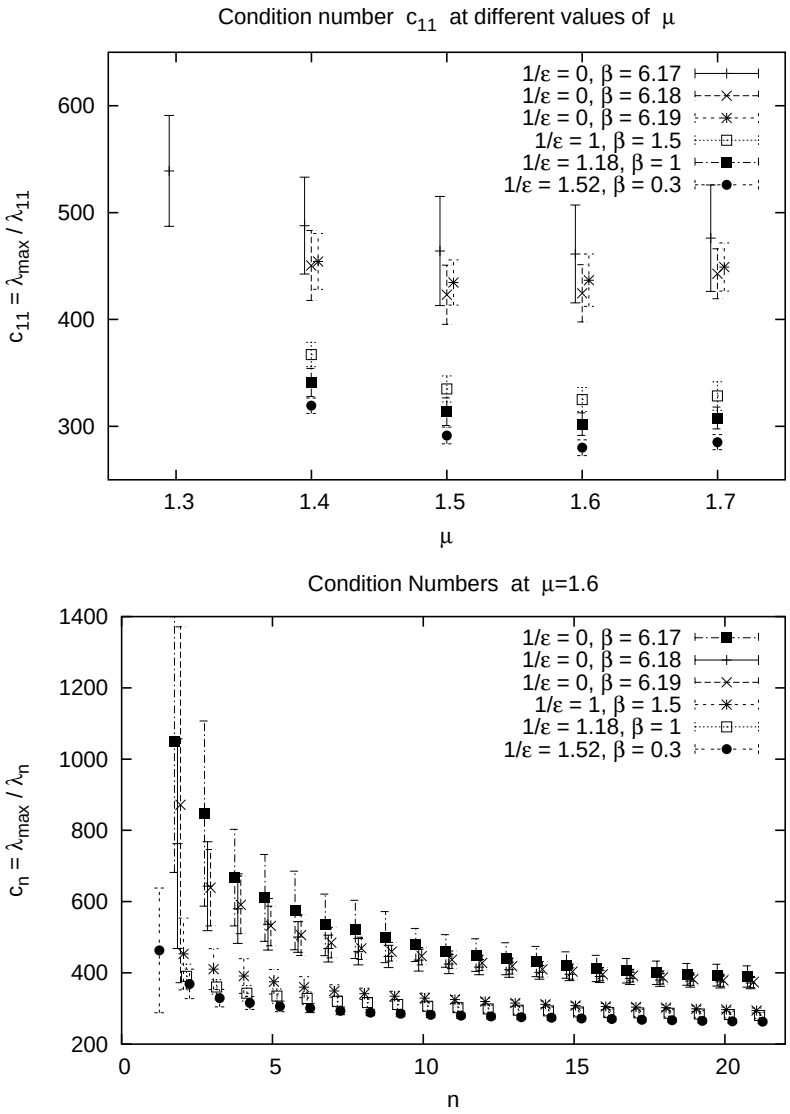

Figure 4: Comparison of the condition number c_{11} for various values of μ (on top), and c_n for running n at $\mu = 1.6$ (below), for different types of gauge actions. (The parameters μ and c_n are defined in eqs. (2.1) and (4.6).)

If n is around 20, then — for the smooth configurations that we considered here — the gain compared to $S_{\rm W}$ is only moderate. However, for the hyperbolic actions $S^{\rm hyp}_{1,\varepsilon}$ the number of these modes can be reduced drastically without much loss in the condition number of the remaining operator. This is in contrast to $S_{\rm W}$, and it matters in applications, since the special treatment of each of these projected modes also takes computation time (although this is typically a minor part of the total computational effort).

4.5 Topological charge stability

For a quick analysis, we used the cooling method [40] to estimate the topological charge.

JHEP03(2006)017

The resulting topological stability over the trajectories is included in tables 1 and 2. In independent tests we evaluated for a subset of the configurations the overlap indices setting $\mu = 1.3$, 1.4, 1.5, 1.6 and 1.7. Since we are dealing with smooth configurations, it does not come as a surprise that we found an excellent agreement of more than 98 % for all these definitions of the topological charge, i.e. the charges obtained with cooling and the overlap index at any of the parameters μ listed up above.[9] Hence the results in the tables are relevant for the overlap index as well.

As a more direct illustration, we show typical histories of the topological charge (defined by cooling) for different parameters in figure 5. To measure the stability of the topological sector, we monitored the number of charge changes normalised by the number of trajectories. We denote this parameter as the "frequency of topological transitions", $f_{\rm top}$, and give results in tables 1 and 2.

As we already mentioned in subsection 4.3, for a fixed $d\tau$ the acceptance rate drops when we increase $1/\varepsilon$ up to 1.64. Although this problem can be alleviated by reducing $d\tau$, it indicates that at this point the system tends to run too often into forbidden regions, beyond the admissibility cutoff. Therefore we also explored an action, which does not have any strictly forbidden plaquette values. For instance, for the actions in eqs. (3.2) and (3.3) the suppression of small plaquette values rises smoothly. Our results for the exponential action $S^{\rm exp}_{\varepsilon,8}$ are collected in table 2. We see that these actions do allow us to render the topology somewhat more stable, and again small HMC steps help us to keep the acceptance rate high. However, it is difficult to fulfil the requirement $r_0/a \lesssim 7$, although we already chose extremely low values for β. Therefore we did not push further into that direction.

Let us add some technical aspects about the evaluation of $f_{\rm top}$. Although measuring the charges by cooling is rather cheap, it could still not be evaluated after each trajectory (since we were dealing with quite long histories). A reliable determination of $f_{\rm top}$ can only be done if the number of trajectories, which are skipped between two measurements of the charge $Q_{\rm top}$, is much less than the typical number of trajectories over which $Q_{\rm top}$ remains constant. It turned out that for $S_{\rm W}$ it was sufficient to cool one configuration in 5 trajectories. For the gauge actions at $1/\varepsilon > 0$, one configuration out of 50 trajectories was typically enough.

The error on $f_{\rm top}$ was estimated only in a crude way. This is done by counting the transitions in 5 sub-histories and taking the standard deviation from these 5 samples. The idea is inspired by the jack-knife method, but the difference is that the sub-histories have to consist of contiguous elements.

Of course, we also need to consider the effect of $1/\varepsilon > 0$ on the autocorrelation time with respect to non-topological quantities. One could be worried that an improved topological stability comes along with a longer autocorrelation for other observables as well. Our consideration of the plaquette value indicates the opposite: its autocorrelation time *decreases* significantly with increasing $1/\varepsilon$, see tables 1 and 2.

[9] On the other hand, if we decrease $\beta_{\rm W}$ for instance to 5.85, the charge $Q_{\rm top}$ depends significantly on the method of its determination [25].

JHEP03(2006)017

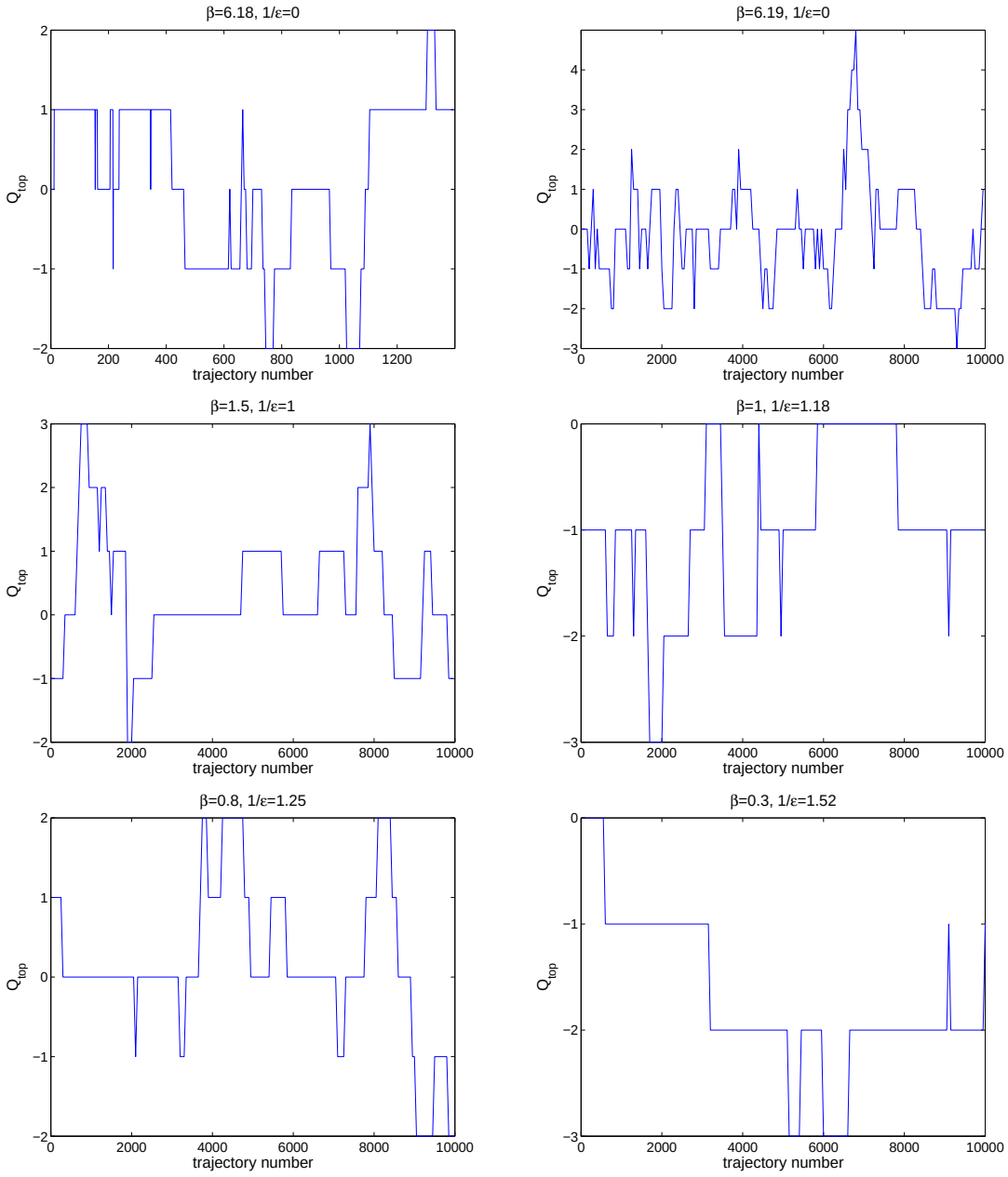

Figure 5: Typical histories of the topological charge for the actions $S_{\rm W}$ (on top) and $S^{\rm hyp}_{\varepsilon,1}$ at various combinations of ε and β, as in table 1. We show results obtained on a 16^4 lattice with the HMC step size $d\tau = 0.1$. We see that an increased $1/\varepsilon$ keeps the charge more and more stable. The charge was measured by cooling once in 50 trajectories, except for the plot at $\beta = 6.18$, where measurements were made every single or every 5 trajectories. Notice, on the other hand, that in the plot at $\beta = 6.19$ the assumption that the separation of measurements is much larger than the typical distance of topology changes is not justified, and the frequency of topological transitions based on this plot would be underestimated.

Another conceivable problem could be bad ergocity properties even within one topological sector as $1/\varepsilon$ is switched on. We checked this by performing simulations from

β	$1/\varepsilon$	$\langle U_P \rangle$	τ^{plaq}	starting point
6	0	0.59371(3)	9.2	cold
6.19	0	0.61181(2)	7.2	cold
0.8	1.25	0.598371(4)	1.1	cold
0.8	1.25	0.598372(4)	1.1	$Q_{\mathrm{top}} = 1$
0.8	1.25	0.598367(4)	1.1	$Q_{\mathrm{top}} = 2$
0.8	1.25	0.598369(4)	1.0	$Q_{\mathrm{top}} = 3$
0.3	1.52	0.601034(3)	0.8	cold
0.3	1.52	0.601028(3)	0.8	$Q_{\mathrm{top}} = 1$

Table 4: Comparison of mean plaquette values $\langle U_P \rangle$ for different parameters and different starting points (out of 10 000 trajectories in a volume 16^4). The decreased plaquette autocorrelations lead to a much more precise determination of $\langle U_P \rangle$. We see a remarkable agreement up to this high precision for different starting points, even in different topological sectors.

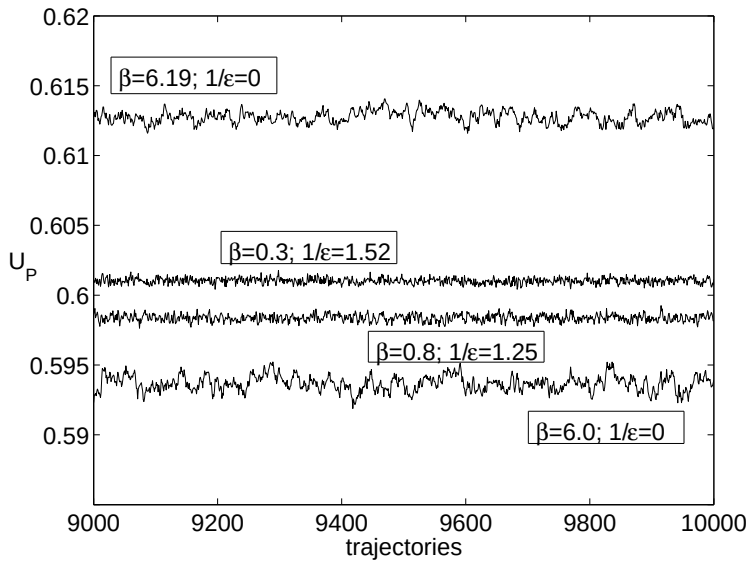

Figure 6: Comparison of short portions of plaquette histories for different combinations of β and ε.

independent starting points and found that the mean plaquette values agree to a very high precision, see table 4 and figure 6.

Of course, such tests should be extended to further observables, but our results for the plaquette value are encouraging.

5. Conclusions

The conservation of the topological charge can be implemented in the lattice gauge action to some extent. There are various obstacles preventing a strict implementation, such as scaling artifacts and the acceptance rate. Still, we succeeded in obtaining long sequences of a stable

JHEP03(2006)017

topological charge, although it cannot be fixed strictly, as expected. Our comparison to the behaviour of the plaquette value suggests that the topological autocorrelation time exceeds by far the autocorrelation of other observables. This property facilitates the collection of many configurations in a specific topological sector, for actions which are perfectly acceptable. We also observed that such actions do not seem to suffer from any conceptual problems. In particular the resulting static potential is fully consistent with the right continuum limit, and it has relatively mild lattice artifacts. We also showed that at least a positive squared transfer matrix can be defined.

Moreover we found benefits of this action for the condition number of the kernel of the overlap operator, which allows for a somewhat faster evaluation with a fixed accuracy. We finally remark that our findings are in accordance with recent results of refs. [32]. Further virtues, in particular in view of the simulations with dynamical quarks, still remain to be explored.

Acknowledgments

We would like to thank M. Creutz, H. Fukaya, S. Hashimoto, M. Ilgenfritz, M. Lüscher, M. Müller-Preußker, K. Ogawa, T. Onogi, R. Sommer and C. Urbach for interesting discussions and helpful remarks. This work was supported by the "Deutsche Forschungsgemeinschaft" through SFB/TR9-03. S. Necco is supported by TMR, EC-Contract No. HPRNCT-2002-00311 (EURIDICE). Part of the computations were performed on the IBM p690 clusters of the "Norddeutscher Verbund für Hoch- und Höchstleistungsrechnen" (HLRN) and at the Forschungszentrum Jülich.

References

[1] K.G. Wilson, *Confinement of quarks*, *Phys. Rev.* **D 10** (1974) 2445.

[2] I. Montvay and G. Münster, *Quantum fields on the lattice*, Cambridge University Press Cambridge 1994.

[3] P. Weisz, *Continuum limit improved lattice action for pure Yang-Mills theory, 1*, *Nucl. Phys.* **B 212** (1983) 1.

[4] M. Lüscher and P. Weisz, *Computation of the action for on-shell improved lattice gauge theories at weak coupling*, *Phys. Lett.* **B 158** (1985) 250; *On-shell improved lattice gauge theories*, *Commun. Math. Phys.* **97** (1985) 59.

[5] Y. Iwasaki, *Renormalization group analysis of lattice theories and improved lattice action, 2. Four-dimensional nonabelian* SU(N) *gauge model*, UTHEP-118;
Y. Iwasaki and T. Yoshié, *Renormalization group improved action for* SU(3) *lattice gauge theory and the string tension*, *Phys. Lett.* **B 143** (1984) 449.

[6] QCDTARO collaboration, P. DeForcrand et al., *Search for effective lattice action of pure QCD*, *Nucl. Phys.* **53** *(Proc. Suppl.)* (1997) 938 [hep-lat/9608094];
T. Takaishi, *Heavy quark potential and effective actions on blocked configurations*, *Phys. Rev.* **D 54** (1996) 1050.

[7] F. Niedermayer, P. Rüfenacht and U. Wenger, *Fixed point gauge actions with fat links: scaling and glueballs*, *Nucl. Phys.* **B 597** (2001) 413 [hep-lat/0007007].

[8] M. Lüscher, *Schwarz-preconditioned HMC algorithm for two-flavour lattice QCD*, *Comput. Phys. Commun.* **165** (2005) 199 [hep-lat/0409106]. *Lattice QCD with light Wilson quarks*, PoS(LAT2005)002 [hep-lat/0509152];
C. Urbach, K. Jansen, A. Shindler and U. Wenger, *HMC algorithm with multiple time scale integration and mass preconditioning*, *Comput. Phys. Commun.* **174** (2006) 87 [hep-lat/0506011].

[9] H. Neuberger, *Exactly massless quarks on the lattice*, *Phys. Lett.* **B 417** (1998) 141 [hep-lat/9707022]; *More about exactly massless quarks on the lattice*, *Phys. Lett.* **B 427** (1998) 353 [hep-lat/9801031].

[10] P.H. Ginsparg and K.G. Wilson, *A remnant of chiral symmetry on the lattice*, *Phys. Rev.* **D 25** (1982) 2649.

[11] P. Hasenfratz, V. Laliena and F. Niedermayer, *The index theorem in QCD with a finite cutoff*, *Phys. Lett.* **B 427** (1998) 125 [hep-lat/9801021];
P. Hasenfratz, *Lattice QCD without tuning, mixing and current renormalization*, *Nucl. Phys.* **B 525** (1998) 401 [hep-lat/9802007].

[12] M. Lüscher, *Exact chiral symmetry on the lattice and the Ginsparg-Wilson relation*, *Phys. Lett.* **B 428** (1998) 342 [hep-lat/9802011].

[13] P. Hernández, K. Jansen and M. Lüscher, *Locality properties of Neuberger's lattice Dirac operator*, *Nucl. Phys.* **B 552** (1999) 363 [hep-lat/9808010].

[14] H. Neuberger, *Bounds on the Wilson Dirac operator*, *Phys. Rev.* **D 61** (2000) 085015 [hep-lat/9911004].

[15] K. Nagao, *An admissibility condition and nontrivial indices on a noncommutative torus*, hep-th/0509034.

[16] J. Gasser and H. Leutwyler, *Thermodynamics of chiral symmetry*, *Phys. Lett.* **B 188** (1987) 477;
H. Neuberger, *A better way to measure f_π in the linear sigma model*, *Phys. Rev. Lett.* **60** (1988) 889;
H. Neuberger, *Soft pions in large boxes*, *Nucl. Phys.* **B 300** (1988) 180;
P. Hasenfratz and H. Leutwyler, *Goldstone boson related finite size effects in field theory and critical phenomena with O(N) symmetry*, *Nucl. Phys.* **B 343** (1990) 241;
F.C. Hansen, *Finite size effects in spontaneously broken* $\mathrm{SU}(N) \times \mathrm{SU}(N)$ *theories*, *Nucl. Phys.* **B 345** (1990) 685;
F.C. Hansen and H. Leutwyler, *Charge correlations and topological susceptibility in QCD*, *Nucl. Phys.* **B 350** (1991) 201;
W. Bietenholz, *Goldstone bosons in a finite volume: the partition function to three loops*, *Helv. Phys. Acta* **66** (1993) 633 [hep-th/9402072].

[17] S. Weinberg, *Phenomenological lagrangians*, *Physica* **96** (1979) 327;
J. Gasser and H. Leutwyler, *Light quarks at low temperatures*, *Phys. Lett.* **B 184** (1987) 83.

[18] H. Leutwyler and A. Smilga, *Spectrum of Dirac operator and role of winding number in QCD*, *Phys. Rev.* **D 46** (1992) 5607;
P.H. Damgaard, M.C. Diamantini, P. Hernández and K. Jansen, *Finite-size scaling of meson propagators*, *Nucl. Phys.* **B 629** (2002) 445 [hep-lat/0112016];

JHEP03(2006)017

P.H. Damgaard, P. Hernández, K. Jansen, M. Laine and L. Lellouch, *Finite-size scaling of vector and axial current correlators*, *Nucl. Phys.* **B 656** (2003) 226 [hep-lat/0211020].

[19] S. Prelovsek and K. Orginos, *Quenched scalar meson correlator with domain wall fermions*, *Nucl. Phys.* **119** *(Proc. Suppl.)* (2003) 822.

[20] W. Bietenholz, K. Jansen and S. Shcheredin, *Spectral properties of the overlap Dirac operator in QCD*, *JHEP* **07** (2003) 033 [hep-lat/0306022];
L. Giusti, M. Lüscher, P. Weisz and H. Wittig, *Lattice QCD in the epsilon-regime and random matrix theory*, *JHEP* **11** (2003) 023 [hep-lat/0309189];
D. Galletly et al., *Random matrix theory and the spectra of overlap fermions*, *Nucl. Phys.* **129** *(Proc. Suppl.)* (2004) 456 [hep-lat/0309030].

[21] L. Del Debbio and C. Pica, *Topological susceptibility from the overlap*, *JHEP* **02** (2004) 003 [hep-lat/0309145];
L. Del Debbio, L. Giusti and C. Pica, *Topological susceptibility in the* SU(3) *gauge theory*, *Phys. Rev. Lett.* **94** (2005) 032003 [hep-th/0407052].

[22] W. Bietenholz, T. Chiarappa, K. Jansen, K.I. Nagai and S. Shcheredin, *Axial correlation functions in the epsilon-regime: a numerical study with overlap fermions*, *JHEP* **02** (2004) 023 [hep-lat/0311012].

[23] L. Giusti, P. Hernández, M. Laine, P. Weisz and H. Wittig, *Low-energy couplings of QCD from topological zero-mode wave functions*, *JHEP* **01** (2004) 003 [hep-lat/0312012].

[24] L. Giusti, P. Hernández, M. Laine, P. Weisz and H. Wittig, *Low-energy couplings of QCD from current correlators near the chiral limit*, *JHEP* **04** (2004) 013 [hep-lat/0402002];
L. Giusti and S. Necco, *Low-mode averaging for baryon correlation functions*, PoS(LAT2005)132 [hep-lat/0510011].

[25] S. Shcheredin, *Simulations of lattice fermions with chiral symmetry in quantum chromodynamics*, hep-lat/0502001;
W. Bietenholz and S. Shcheredin, *Relating chiral perturbation theory and QCD simulations with overlap hypercube fermions*, *Rom. J. Phys.* **50** (2005) 249 [hep-lat/0502010];
W. Bietenholz and S. Shcheredin, *Overlap hypercube fermions in QCD with light quarks*, PoS(LAT2005)138 [hep-lat/0508016];
S. Shcheredin and W. Bietenholz, *Low energy constants from the zero mode contribution to the pseudo-scalar correlator*, PoS(LAT2005)134 [hep-lat/0508034].

[26] H. Fukaya, S. Hashimoto and K. Ogawa, *Low-lying mode contribution to the quenched meson correlators in the epsilon-regime*, *Prog. Theor. Phys.* **114** (2005) 451 [hep-lat/0504018];
H. Fukaya, S. Hashimoto and K. Ogawa, *Meson correlators in a finite volume near the chiral limit*, PoS(LAT2005)133 [hep-lat/0510049];
K. Ogawa and S. Hashimoto, *Effect of low-lying fermion modes in the epsilon-regime of QCD*, *Prog. Theor. Phys.* **114** (2005) 609 [hep-lat/0505017].

[27] J. Wennekers and H. Wittig, *On the renormalized scalar density in quenched QCD*, *JHEP* **09** (2005) 059 [hep-lat/0507026];
L. Giusti, P. Hernández, M. Laine, C. Pena, J. Wennekers and H. Wittig, *On the determination of low-energy constants for* $\Delta S = 1$ *transitions*, PoS(LAT2005)344 [hep-lat/0510033].

[28] M. Lüscher, *Abelian chiral gauge theories on the lattice with exact gauge invariance*, *Nucl. Phys.* **B 549** (1999) 295 [hep-lat/9811032]; *Weyl fermions on the lattice and the non-abelian gauge anomaly*, *Nucl. Phys.* **B 568** (2000) 162 [hep-lat/9904009].

JHEP03(2006)017

[29] H. Fukaya and T. Onogi, *Lattice study of the massive Schwinger model with theta term under Lüscher's 'admissibility' condition*, *Phys. Rev.* **D 68** (2003) 074503 [hep-lat/0305004]; *theta vacuum effects on the chiral condensation and the η' meson correlators in the two-flavor massive QED_2 on the lattice*, *Phys. Rev.* **D 70** (2004) 054508 [hep-lat/0403024].

[30] S. Shcheredin, W. Bietenholz, K. Jansen, K.-I. Nagai, S. Necco and L. Scorzato, *Testing a topology conserving gauge action in QCD*, *Nucl. Phys.* **140** *(Proc. Suppl.)* (2005) 779 [hep-lat/0409073];
XLF collaboration, W. Bietenholz et al., *Lattice gauge actions for fixed topology*, *AIP Conf. Proc.* **756** (2005) 248 [hep-lat/0412017];
K.-I. Nagai, K. Jansen, W. Bietenholz, L. Scorzato, S. Necco and S. Shcheredin, *Testing topology conserving gauge actions for lattice QCD*, PoS(LAT2005)283 [hep-lat/0509170].

[31] H. Fukaya, T. Onogi, S. Hashimoto, T. Hirohashi and K. Ogawa, *Parameter dependence of the topology change and the scaling properties of the topology conserving gauge action*, PoS(LAT2005)317 [hep-lat/0509184].

[32] H. Fukaya et al., *Overlap fermion with the topology conserving gauge action*, PoS(LAT2005)123 [hep-lat/0510095];
H. Fukaya, S. Hashimoto, T. Hirohashi, K. Ogawa and T. Onogi, *Topology conserving gauge action and the overlap-Dirac operator*, *Phys. Rev.* **D 73** (2006) 014503 [hep-lat/0510116].

[33] M. Creutz, *Positivity and topology in lattice gauge theory*, *Phys. Rev.* **D 70** (2004) 091501 [hep-lat/0409017].

[34] R. Sommer, *A new way to set the energy scale in lattice gauge theories and its applications to the static force and α_s in* SU(2) *Yang-Mills theory*, *Nucl. Phys.* **B 411** (1994) 839 [hep-lat/9310022].

[35] P. Marenzoni, L. Pugnetti and P. Rossi, *Measure of autocorrelation times of local Hybrid Monte Carlo algorithm for lattice QCD*, *Phys. Lett.* **B 315** (1993) 152 [hep-lat/9306013].

[36] ALPHA collaboration, M. Guagnelli, R. Sommer and H. Wittig, *Precision computation of a low-energy reference scale in quenched lattice QCD*, *Nucl. Phys.* **B 535** (1998) 389 [hep-lat/9806005].

[37] S. Necco and R. Sommer, *The $N_f = 0$ heavy quark potential from short to intermediate distances*, *Nucl. Phys.* **B 622** (2002) 328 [hep-lat/0108008].

[38] S. Necco, *Universality and scaling behavior of RG gauge actions*, *Nucl. Phys.* **B 683** (2004) 137 [hep-lat/0309017]; *The static quark potential and scaling behavior of* SU(3) *lattice Yang-Mills theory*, hep-lat/0306005.

[39] W. Bietenholz, *Solutions of the Ginsparg-Wilson relation and improved domain wall fermions*, *Eur. Phys. J.* **C 6** (1999) 537 [hep-lat/9803023]; *Convergence rate and locality of improved overlap fermions*, *Nucl. Phys.* **B 644** (2002) 223 [hep-lat/0204016];
W. Bietenholz and I. Hip, *The scaling of exact and approximate Ginsparg-Wilson fermions*, *Nucl. Phys.* **B 570** (2000) 423 [hep-lat/9902019];
MILC collaboration, T.A. DeGrand, *A variant approach to the overlap action*, *Phys. Rev.* **D 63** (2001) 034503 [hep-lat/0007046];
W. Kamleh, D.H. Adams, D.B. Leinweber and A.G. Williams, *Accelerated overlap fermions*, *Phys. Rev.* **D 66** (2002) 014501 [hep-lat/0112041];
S. Dürr, C. Hoelbling and U. Wenger, *Filtered overlap: speedup, locality, kernel non-normality and $Z_A \sim 1$*, *JHEP* **09** (2005) 030 [hep-lat/0506027].

JHEP03(2006)017

[40] E.-M. Ilgenfritz, M.L. Laursen, G. Schierholz, M. Müller-Preußker and H. Schiller, *First evidence for the existence of instantons in the quantized* SU(2) *lattice vacuum*, *Nucl. Phys.* **B 268** (1986) 693.